Research Square

Preprints are preliminary reports that have not undergone peer review.
They should not be considered conclusive, used to inform clinical practice,
or referenced by the media as validated information.

A Diagnostic Model for Central Precocious Puberty in Girls Based on Ultrasonic Bone Age and Clinical Indicators

Minghang Lin
Fuqing City Hospital Affiliated to Fujian Medical University
Yiming Su
The First Affiliated Hospital of Xiamen University, School of Medicine, Xiamen University
Qianni Chen
Fuqing City Hospital Affiliated to Fujian Medical University
Lei Yan
The First Affiliated Hospital of Fujian Medical University
Mei He
Fuqing City Hospital Affiliated to Fujian Medical University
Gong He
Fuqing City Hospital Affiliated to Fujian Medical University
Shuqiang Chen
chenshu0518@163.com

Fuzhou University Affiliated Provincial Hospital

Research Article

Keywords: Central Precocious Puberty, Diagnostic Model, Ultrasonic Bone Age, Clinical Indicators

Posted Date: May 7th, 2026

DOI: https://doi.org/10.21203/rs.3.rs-9473736/v1

License: This work is licensed under a Creative Commons Attribution 4.0 International License.
Read Full License

Additional Declarations: No competing interests reported.

Abstract

Background

Central precocious puberty (CPP) is a common pediatric endocrine disorder in girls. The diagnostic gold standard, the GnRH stimulation test, is invasive, limiting its widespread use. Ultrasound-based bone age assessment is radiation-free, but its diagnostic value within an integrated model remains unvalidated.

Objective

To develop and validate a model integrating ultrasound bone age advancement (ΔBA_OA), pelvic ultrasound indicators, and clinical-biochemical markers for non-invasive differential diagnosis of CPP in girls.

Methods

269 girls initially diagnosed with precocious puberty were enrolled. Based on GnRH stimulation test results, they were divided into CPP (n = 66) and non-CPP (n = 203) groups. Clinical data, pelvic ultrasound parameters, hormone levels, and ultrasound bone age parameters were collected. Independent predictors were identified using logistic regression. Model performance was assessed by AUC, calibration curve, and decision curve analysis (DCA).

Results

ΔBA_OA (OR = 61.05), basal LH (OR = 8.76), and IGF-1 (OR = 1.02) were independent predictors (all $P < 0.001$). Standardized coefficients confirmed comparable contributions from ΔBA_OA (β = 0.675) and LH (β = 0.637). The model achieved an AUC of 0.972 (95%CI: 0.950–0.993). Calibration showed good agreement (MAE = 0.016), and DCA indicated positive net benefit.

Conclusion

The proposed model incorporating ultrasound bone age parameter ΔBA_OA with clinical and biochemical markers demonstrates good discriminative ability and clinical utility for non-invasive differential diagnosis of CPP in girls. Quantitative ultrasound bone age assessment may serve as a promising complementary tool, supporting a radiation-free, multidimensional diagnostic system. External validation in multicenter, large-sample studies is warranted.

Introduction

Central precocious puberty (CPP) is a common pediatric endocrine disorder characterized by premature activation of the hypothalamic-pituitary-gonadal axis (HPGA), leading to increased pulsatile secretion of gonadotropin-releasing hormone (GnRH) and subsequently resulting in early sexual development and accelerated bone maturation(1, 2). In girls, CPP manifests as the development of secondary sexual characteristics, such as breast development before 7.5 years of age or menarche before 10.0 years of age(3). The incidence of CPP in girls is approximately ten times higher than in boys, and has been increasing steadily in recent years (4). Without timely diagnosis and intervention, CPP may compromise final adult height and lead to psychological and behavioral problems.

Currently, the diagnosis of CPP relies on clinical manifestations, bone age assessment, pelvic ultrasound, and the GnRH stimulation test. The GnRH stimulation test is considered the gold standard for the clinical diagnosis of CPP(5, 6). However, this test is invasive, time-consuming, costly, and associated with poor patient compliance, which limits its widespread clinical application. Bone age assessment is an important indicator reflecting skeletal maturity and aiding in the diagnosis of CPP. Traditional bone age assessment primarily relies on left hand-wrist radiography. Although widely used, this method carries the risk of ionizing radiation exposure, and its accuracy depends to some extent on the experience of the interpreting physician (7, 8).

In recent years, ultrasound technology has been increasingly applied in pediatric endocrinology due to its non-invasive nature, absence of ionizing radiation, and real-time dynamic imaging capabilities. Pelvic ultrasound (for assessing uterine and ovarian morphology) has been incorporated into the routine evaluation of CPP (9). However, the potential of ultrasound for assessing skeletal maturity—a direct reflection of the core pathophysiological process of CPP—has not been fully explored. Studies have shown that ultrasound can clearly visualize the morphology of epiphyseal cartilage and ossification centers, and objectively assess skeletal maturity by measuring quantitative parameters such as the ossification angle and ossification rate. These ultrasound-based bone age parameters may reflect the promoting effect of sex hormones on the growth plate more sensitively than a single bone age reading alone (10). Although sporadic studies have explored the correlation of individual ultrasound parameters with bone age or CPP, there remains a lack of research that systematically integrates multi-dimensional quantitative ultrasound bone age indicators with conventional clinical parameters to construct a comprehensive diagnostic model (11).

The present study aims to develop a comprehensive predictive model for the differential diagnosis of CPP in girls by innovatively integrating a quantitative ultrasound bone age assessment system with pelvic ultrasound parameters, basic clinical and biochemical indicators. By evaluating the diagnostic performance, calibration, and clinical utility of this model, we expect to provide a new and effective tool for the early, non-invasive, and accurate diagnosis of CPP, thereby optimizing clinical management pathways and reducing unnecessary invasive procedures and radiation exposure.

Materials and Methods

2.1 Study Participants

A total of 269 girls who were initially diagnosed with precocious puberty at a single hospital, between April 1, 2024 and October 18, 2025 were consecutively enrolled. The study protocol was approved by the institutional ethics committee (approval number blinded for review), and written informed consent was obtained from the guardians of all participating girls.

2.2 Inclusion and Exclusion Criteria

Inclusion Criteria:

(1) Clinical presentation of breast development (Tanner stage ≥ B2) before 7.5 years of age or menarche before 10.0 years of age;

(2) Completion of the gonadotropin-releasing hormone agonist (GnRHa) stimulation test. A positive GnRHa stimulation test was defined as a peak LH level ≥ 5 IU/L or a peak LH/FSH ratio ≥ 0.6;

(3) Undergoing pelvic ultrasound and ultrasound-based bone age assessment within one week after completion of the GnRHa stimulation test.

Exclusion Criteria:

(1) Previous treatment with GnRHa analogues;

(2) Comorbid endocrine disorders (e.g., thyroid dysfunction, congenital adrenal hyperplasia) or known intracranial organic lesions;

(3) Structural or pathological changes in the wrist or knee joints due to trauma, infection, tumor, or other causes.

2.3 Clinical Data Collection

Baseline clinical data were recorded for all enrolled girls, including age at presentation, duration of sexual development, height, and weight. Body mass index (BMI) was calculated. Breast Tanner staging was assessed and recorded by a pediatric endocrinologist.

2.4 Laboratory Measurements

Morning fasting venous blood samples were collected from the participants. Basal levels of estradiol (E2), luteinizing hormone (LH), follicle-stimulating hormone (FSH), insulin-like growth factor 1 (IGF-1), and thyroid-stimulating hormone (TSH) were measured and recorded.

2.5 Pelvic Ultrasound Examination

Pelvic ultrasound was performed using an Aixplorer ultrasound system (SuperSonic Imagine, France) equipped with a convex array probe (2.5–5 MHz) using a preset abdominal imaging mode. Participants

were instructed to drink sufficient water to achieve a full bladder and were placed in the supine position. The probe was used to obtain clear longitudinal and transverse images of the uterus and both ovaries. The length, anteroposterior diameter, and transverse diameter of the uterus and both ovaries were measured and recorded. The number of follicles and the maximum follicle diameter in both ovaries were also recorded. All measurements were taken three times, and the average value was used for analysis.

2.6 Ultrasound Bone Age Image Acquisition and Parameter Measurement

2.6.1 Ultrasound Bone Age Image Acquisition

Ultrasound bone age images were acquired using the same Aixplorer system equipped with a high-frequency linear array probe (5–12 MHz) using a preset musculoskeletal imaging mode. All images were obtained by a single experienced sonographer with more than five years of relevant experience who was blinded to the participants' group assignment and clinical information. The specific scanning sites and positions were as follows:

- **Distal radius**: The participant was placed in the supine position with the left forearm in a neutral position. The probe was placed on the coronal plane of the radial styloid process.
- **Distal ulna**: The participant was placed in the supine position with the left forearm pronated. The probe was placed on the coronal plane of the ulnar styloid process.
- **Medial femoral epicondyle**: The participant was placed in the supine position with the left knee slightly abducted. The probe was placed on the coronal plane of the medial femoral condyle, and images were acquired after clearly visualizing the medial collateral ligament and medial epicondyle structures.

2.6.2 Ultrasound Bone Age Parameter Measurement and Analysis

Acquired images were measured in a blinded manner by two other sonographers, each with more than five years of experience. The measurement parameters and methods were as follows:

An extension line was drawn along the outer margin of the strong echo band of the diaphysis. A perpendicular line was drawn from the farthest point of the diaphysis to this extension line, and their intersection was defined as the starting point. A tangent line was drawn from this starting point to the strong echo band of the secondary ossification center. The angle between this tangent line and the diaphysis extension line was measured as the ossification angle (OA) for that site (Fig. 1). The OA was measured separately for the radius, ulna, and femur, and the sum of the three angles was recorded as the total ossification angle. Bone age based on the ossification angle (OA_BA) was calculated from the total ossification angle, and bone age advancement (ΔBA_OA) was calculated as: ΔBA_OA = OA_BA – chronological age (12).

2.7 Statistical Analysis

Statistical analyses were performed using SPSS Statistics version 22.0 (IBM, USA). Normally distributed continuous data were expressed as mean ± standard deviation, non-normally distributed data as median (interquartile range), and categorical data as frequency (percentage). The intraclass correlation coefficient (ICC) was used to assess inter-observer agreement for ultrasound parameter measurements between the two sonographers, with an ICC > 0.75 indicating good agreement.

Univariate logistic regression analysis was performed to preliminarily screen for significant variables, with disease group as the dependent variable and all candidate variables as independent variables. Variables with $P < 0.05$ in the univariate analysis were then entered into a multivariate logistic regression model to identify independent predictors. Results are presented as odds ratios (OR) with 95% confidence intervals (CI). A predictive model was constructed based on the results of the multivariate logistic regression analysis.

Discriminatory ability was assessed by plotting receiver operating characteristic (ROC) curves and calculating the area under the curve (AUC) with its 95% CI. Calibration curves were plotted using R software (version 4.2.0, R Foundation for Statistical Computing, Austria) to evaluate the agreement between predicted probabilities and observed outcomes, and the Hosmer-Lemeshow goodness-of-fit test was performed. Decision curve analysis (DCA) was performed to evaluate the net clinical benefit of the model across different threshold probabilities. Finally, a nomogram was constructed based on the regression coefficient weights of each independent predictor to enable individualized risk prediction.

Results

3.1 Baseline Characteristics of the Study Participants

A total of 298 girls initially diagnosed with precocious puberty were enrolled in this study. After excluding 23 girls who had previously received GnRHa analogue therapy and 6 girls with comorbid endocrine disorders (e.g., thyroid dysfunction), 269 girls were finally included in the analysis. Their mean chronological age was 8.34 ± 1.35 years. Based on the GnRH stimulation test results, 66 girls (24.5%) were definitively diagnosed with central precocious puberty (CPP), and 203 girls (75.5%) were classified into the non-CPP group. There were no statistically significant differences between the two groups in terms of age at presentation or the distribution of breast Tanner stages ($P > 0.05$). However, BMI was significantly higher in the CPP group than in the non-CPP group. Detailed information is presented in Table 1.

Table 1
Baseline Characteristics and Comparative Analysis of Girls with Central Precocious Puberty (CPP) and non-CPP

Variable	Total (n = 269)	CPP (n = 66)	Non-CPP (n = 203)	P-value
Demographics				
CA (years)	8.34 ± 1.35	8.19 ± 1.18	8.39 ± 1.40	0.315
BMI (kg/m²)	16.98 ± 3.48	18.00 ± 4.07	16.65 ± 3.20	0.016
B_Tanner(n)				0.261
I	0	0	0	
II	186	52	134	
III	68	10	58	
IV	15	4	11	
BA & Maturation				
BA_OA (years)	9.25 ± 1.53	10.03 ± 1.30	8.99 ± 1.52	< 0.001
ΔBA_OA (years)	0.91 ± 1.20	2.12 ± 0.99	0.51 ± 0.98	< 0.001
UL (mm)	21.51 ± 5.08	24.50 ± 5.80	20.53 ± 4.42	< 0.001
UV (mL)	5.14 ± 5.17	4.91 ± 4.50	5.22 ± 5.38	0.833
ET (mm)	1.16 ± 1.59	1.47 ± 1.92	1.06 ± 1.46	0.331
Ovarian & Follicular				
LOV (mL)	3.75 ± 2.26	3.51 ± 1.97	3.82 ± 2.34	0.529
ROV (mL)	4.34 ± 2.66	4.55 ± 2.82	3.69 ± 1.97	0.032
No. of Follicles _L(n)	3.32 ± 2.27	3.71 ± 2.40	3.20 ± 2.22	0.088
No. of Follicles _R(n)	3.99 ± 2.55	4.48 ± 2.98	3.83 ± 2.38	0.194
Hormonal				
E2 (pg/mL)	16.78 ± 14.76	25.84 ± 24.20	13.83 ± 8.06	< 0.001
IGF-1 (ng/mL)	227.00 ± 79.32	292.45 ± 102.06	205.73 ± 56.04	< 0.001
TSH (μIU/mL)	2.41 ± 1.26	2.58 ± 1.39	2.36 ± 1.21	0.229
LH (IU/L)	0.40 ± 0.93	0.99 ± 1.65	0.21 ± 0.35	< 0.001
FSH (IU/L)	2.62 ± 1.59	3.34 ± 1.96	2.34 ± 1.37	< 0.001

3.2 Comparison of Imaging and Laboratory Indicators

Comparison of imaging and laboratory indicators between the two groups showed that the CPP group had significantly higher values than the non-CPP group in bone age (BA_OA), bone age advancement (ΔBA_OA), uterine length (UL), right ovarian volume (ROV), and basal serum levels of E2, IGF-1, LH, and FSH (all $P < 0.05$). No statistically significant differences were observed between the two groups in uterine volume, endometrial thickness, number of ovarian follicles, or TSH level (all $P > 0.05$). Detailed information is presented in Table 1.

3.3 Multivariate Logistic Regression Analysis and Diagnostic Model Construction

Based on the variables that were statistically significant in the univariate analysis, a multivariate logistic regression model was constructed using forward stepwise selection. The results showed that ΔBA_OA, IGF-1, and LH were independent predictors of CPP in girls (all $P < 0.05$) (Table 2). Accordingly, the following prediction equation was established:

Table 2
Multivariate Logistic Regression Analysis of Independent Predictors for Central Precocious Puberty

Variable	B	P-value	Exp(B)	95% Confidence Interval of Exp(B)
ΔBA_OA	4.112	< 0.001	61.046	16.270–229.059
IGF-1	0.022	< 0.001	1.022	1.011–1.033
LH	2.171	0.001	8.764	2.515– 30.545
Constant	-12.949	< 0.001	–	–

$$\text{Logit}(P) = -12.949 + 4.112 \times \Delta BA_OA + 0.022 \times IGF\text{-}1 + 2.171 \times LH$$

Among these, ΔBA_OA, LH, and IGF-1 were risk factors for CPP, with odds ratios (95% CI) of 61.046 (16.270–229.059), 8.764 (2.515–30.545), and 1.022 (1.011–1.033), respectively. To compare the relative importance of predictors measured on different scales, standardized regression coefficients were calculated. The standardized β values for ΔBA_OA, LH, and IGF-1 were 0.675, 0.637, and 0.005, respectively, indicating that all three variables made independent contributions to the model (all $P < 0.05$).

3.4 Performance Evaluation of the Diagnostic Model

To evaluate the diagnostic performance of the model, an ROC curve was plotted. The area under the curve (AUC) for predicting CPP was 0.972 (95% CI: 0.950–0.993), indicating good discriminative ability (Fig. 2). The calibration curve showed good agreement between predicted probabilities and observed outcomes, with a mean absolute error (MAE) of 0.016 (Fig. 3). Decision curve analysis (DCA) demonstrated that using the model for clinical decision-making provided a higher net benefit across a wide range of threshold probabilities, indicating favorable clinical utility (Fig. 4).

3.5 Nomogram Visualization of the Model

To facilitate individualized risk assessment in clinical practice, the three independent predictors were incorporated into a nomogram model (Fig. 5). Each variable was assigned a different point value (Points) based on its regression coefficient. The total points ranged from 0 to 240, corresponding to the linear predictor and the probability of the outcome risk (Risk of Outcome). For example, after calculating the total points based on a child's bone age advancement and hormone levels, the corresponding probability of CPP can be directly read from the nomogram, thereby achieving risk quantification.

Discussion

In this study, we successfully constructed and validated a logistic regression model for the differential diagnosis of central precocious puberty (CPP) in girls by systematically integrating innovative quantitative ultrasound bone age parameters, pelvic ultrasound morphological indicators, and conventional clinical and biochemical markers. The model demonstrated good diagnostic performance (AUC = 0.972), as well as favorable calibration and clinical utility. Among the predictors, ΔBA_OA, LH, and IGF-1 were identified as independent factors. This study is the first to successfully integrate a systematic quantitative ultrasound bone age assessment system into a diagnostic model for CPP, providing a powerful new tool for the non-invasive, multidimensional evaluation of this disorder.

Pathophysiological Basis and Diagnostic Value of Ultrasound Bone Age Parameters

The key role of ultrasound bone age assessment in this model is closely aligned with the core pathophysiology of CPP. The essence of CPP is premature activation of the hypothalamic-pituitary-gonadal axis (HPGA), leading to elevated sex hormone (particularly estrogen) levels. Estrogen directly accelerates skeletal maturation and bone age advancement by promoting the proliferation, maturation, and apoptosis of epiphyseal chondrocytes and enhancing endochondral ossification (13–15). The ultrasound parameter used in this study—the ossification angle, which reflects the extent of secondary ossification center expansion relative to the diaphysis—sensitively and quantitatively captures the micro- and macroscopic morphological changes associated with endochondral ossification (12). As a composite indicator, ΔBA_OA quantifies the deviation of this accelerated maturation from chronological age. Its emergence as a strong predictor provides direct radiological evidence of the promoting effect of sex hormones on the skeletal system, offering an objective biological marker for CPP diagnosis beyond hormone levels alone. Compared with previous diagnostic models that relied primarily on pelvic gonadal morphology or a single bone age reading, our model provides a functional imaging dimension that more directly reflects the pathophysiological process (16).

Interpretation of the Role of Clinical and Biochemical Predictors

The inclusion of the other independent predictors in the model also has clear clinical and physiological significance. Basal LH level is one of the most direct serological markers of central HPGA activation. Its predictive value (OR = 8.764, 95% CI: 2.515–30.545) is highly consistent with the logic of the diagnostic

gold standard (GnRH stimulation test), confirming its central role in the model. Elevated serum IGF-1 levels reflect the synergistic activation of the growth hormone–insulin-like growth factor axis driven by sex hormones, which is closely related to the growth acceleration observed in children with CPP (17). Although the standardized coefficient for IGF-1 was small, it remained statistically significant in the multivariate model ($P < 0.001$). This modest effect size may reflect the fact that IGF-1 is more closely related to linear growth acceleration than to central pubertal activation per se (18). Nevertheless, incorporating IGF-1 into the model enhanced its clinical comprehensiveness without materially affecting model performance. As an ultrasound bone age parameter, ΔBA_OA showed the strongest predictive power in this model (OR = 61.046, 95% CI: 16.270–229.059), suggesting that ultrasound bone age assessment based on the ossification angle may provide unique imaging evidence for the diagnosis of CPP.

Comparison with Existing Diagnostic Methods and Model Advantages

Compared with the diagnostic gold standard (GnRH stimulation test), our model demonstrated comparable discriminative ability (AUC = 0.972) while offering significant advantages, including non-invasiveness, absence of radiation, rapidity, and low cost. Compared with previous models that used only pelvic ultrasound or conventional bone age, the innovation of our model lies in the construction of a multimodal quantitative assessment system that encompasses both skeletal maturity (ultrasound bone age) and endocrine activity (LH and IGF-1), thereby achieving higher diagnostic accuracy and information richness (19–22)[17–20]. Standardized regression coefficients showed comparable contributions from ΔBA_OA ($\beta = 0.675$) and LH ($\beta = 0.637$), confirming that ultrasound bone age provides independent predictive information complementary to hormone levels. The development of a visual nomogram successfully transformed the complex multifactor model into a convenient clinical decision-making tool, enabling individualized risk prediction and greatly enhancing its potential for application in primary care or outpatient screening settings.

Clinical Significance and Application Prospects

Our model and nomogram have clear potential for clinical translation. They are expected to optimize current diagnostic and management pathways: for girls with clinically suspected precocious puberty, the model can first be applied for initial risk assessment. For children predicted to be at low risk, enhanced follow-up observation could be undertaken, avoiding unnecessary invasive tests (e.g., GnRH stimulation test) and radiation exposure (repeated bone age radiography). For children at moderate to high risk, the GnRH stimulation test could be performed more selectively to confirm the diagnosis. This risk-stratified triage strategy could help optimize the allocation of medical resources, reduce the economic and psychological burden on families, and promote early, precise intervention for CPP.

Limitations

This study has several limitations. First, although the model showed good discriminative ability (AUC = 0.972), this performance may be influenced to some extent by overfitting, particularly given the relatively

limited sample size (269 cases) and the number of predictors. The model's performance needs to be confirmed in independent external validation cohorts to assess its generalizability. Second, this is a single-center study, and the representativeness of the sample may be limited. The model's performance requires external validation in larger, multicenter prospective cohorts to confirm its generalizability. Third, the model is currently applicable only to girls; its applicability to the diagnosis of CPP in boys requires further investigation. Finally, although the measurement of ultrasound bone age parameters was standardized and demonstrated good inter-observer agreement, its accuracy still depends to some extent on the operator's experience. Future development of artificial intelligence-assisted automated measurement and analysis systems holds promise for further improving the objectivity, reproducibility, and dissemination efficiency of this technique.

Conclusion

In this study, we constructed and preliminarily validated a comprehensive model integrating ultrasound bone age (ΔBA_OA), clinical, and biochemical indicators to assist in the differential diagnosis of central precocious puberty in girls. The model demonstrated preliminary discriminative ability in this study cohort; however, its performance requires external validation in multicenter, large-sample prospective studies. Quantitative ultrasound bone age assessment may have complementary value in the auxiliary diagnosis of CPP, providing preliminary evidence for the establishment of a radiation-free, multidimensional diagnostic evaluation system.

Declarations

Conflicts Of Interest: The authors have no conflicts of interest to declare.

Ethical Statement: The authors are accountable for all aspects of the work in ensuring that questions related to the accuracy or integrity of any part of the work are appropriately investigated and resolved. The trial was conducted in accordance with the Declaration of Helsinki and its subsequent amendments. The study was approved by the local Institutional Review Board, and informed consent was obtained from all individual participants.

Author Contribution

M.H.L. and S.Q.C. contributed to the conception and design of the study. S.Q.C. provided administrative support. Y.M.S. and Q.N.C. provided study materials or patients. M.H.L., L.Y., and G.H. performed data collection and assembly. M.H.L., Q.N.C., and Y.M.S. conducted data analysis and interpretation. All authors contributed to manuscript writing and reviewed the final version of the manuscript.

Acknowledgement

The authors wish to thank the staff of the Ultrasound Department at the participating institution for their invaluable contribution to this study. Their dedicated efforts in case collection were instrumental to the successful completion of this research.

References

1. Amanda Veiga C, Leticia Guimarães dS, Leila Cristina Pedroso dP, Iara Regina Siqueira, Sandra Pinho L (2021) S. Diagnosis and management of precocious sexual maturation: an updated review. Eur J Pediatr. ;180(10)
2. DeAnna BB, Lindsey A, L-A, Andrew AB (2013) Sexual precocity and its treatment. World J Pediatr. ;9(2)
3. Subspecialty Group of, Endocrinologic H (2023) Metabolic Diseases tSoPCMA, Editorial Board CJoP. [Expert consensus on the diagnosis and treatment of central precocious puberty(2022)]. Zhonghua Er Ke Za Zhi 61(1):16–22
4. Joshua M-S, Lawrence AS (2022) A review of the genetics and epigenetics of central precocious puberty. Front Endocrinol (Lausanne). ;13(0)
5. Tao Y, Si C, Li H, Han J, Hou H, Yang M (2020) Effect of gonadotropin-releasing hormone analog on ovarian reserve in children with central precocious puberty. Ann Palliat Med 9(1):53–62
6. Latronico AC, Brito VN, Carel JC (2016) Causes, diagnosis, and treatment of central precocious puberty. Lancet Diabetes Endocrinol 4(3):265–274
7. Ana LC, Frederick W 2nd (2017) S. Bone Age: A Handy Tool for Pediatric Providers. Pediatrics. ;140(6)
8. Monika P-P, Kamila M-D, Elżbieta M, Mieczysław S, Elżbieta J (2020) Traditional and New Methods of Bone Age Assessment-An Overview. J Clin Res Pediatr Endocrinol. ;13(3)
9. You J, Cheng X, Li X, Li M, Yao L, Luo F et al (2021) Clinical risk score for central precocious puberty among girls with precocious pubertal development: a cross sectional study. BMC Endocr Disord 21(1):75
10. Jie W, Ying Z, Qunqun F, Chao Z (2020) Summation of Ossification Ratios of Radius, Ulna and Femur: A New Parameter to Evaluate Bone Age by Ultrasound. Ultrasound Med Biol. ;46(7)
11. Jie W, Ying Z, Qunqun F, Pin L, Kai H, Chao Z (2021) Statistical Confirmation of a Method of US Determination of Bone Age. Radiology. ;300(1)
12. Minghang L, Lei Y, Haiying H, Qianni C, Mei H, Shuqiang C (2026) Preliminary study on ultrasound-based quantitative assessment of epiphyseal ossification angle for bone age evaluation in children. Quant Imaging Med Surg. ;16(2)
13. Brito VN, Canton APM, Seraphim CE, Abreu AP, Macedo DB, Mendonca BB et al (2023) The Congenital and Acquired Mechanisms Implicated in the Etiology of Central Precocious Puberty. Endocr Rev 44(2):193–221

14. Vincenzo R, Elda K, Cesare C (2015) The endocrine role of estrogens on human male skeleton. Int J Endocrinol 2015:0
15. Mari S, Yukihiro H (2022) Factors affecting prepubertal and pubertal bone age progression. Front Endocrinol (Lausanne). ;13(0)
16. Calcaterra V, Klersy C, Vinci F, Regalbuto C, Dobbiani G, Montalbano C et al (2020) Rapid progressive central precocious puberty: diagnostic and predictive value of basal sex hormone levels and pelvic ultrasound. J Pediatr Endocrinol Metab 33(6):785–791
17. Escagedo PD, Deal CL, Dwyer AA, Hauschild M (2021) Insulin-like Growth Factor 1, but Not Insulin-Like Growth Factor-Binding Protein 3, Predicts Central Precocious Puberty in Girls 6–8 Years Old: A Retrospective Study. Horm Res Paediatr 94(1–2):44–51
18. Yuping L, Yaying C, Meng S, Xiaojing H, Mengmeng L (2023) Analysis of serum insulin-like growth factor-1, fibroblast growth factor 23, and Klotho levels in girls with rapidly progressive central precocious puberty. Eur J Pediatr. ;182(11)
19. Cleemann Wang A, Hagen CP, Johannsen TH, Madsen AG, Cleemann LH, Christiansen P et al (2024) Differentiation of Idiopathic Central Precocious Puberty From Premature Thelarche Using Principal Component Analysis. J Clin Endocrinol Metab 109(2):370–379
20. Zou P, Zhang L, Zhang R, Wang C, Lin X, Lai C et al (2023) Development and Validation of a Combined MRI Radiomics, Imaging and Clinical Parameter-Based Machine Learning Model for Identifying Idiopathic Central Precocious Puberty in Girls. J Magn Reson Imaging 58(6):1977–1987
21. Quynh Thi Vu H, Nguyen Quoc Khanh L, Shih-Yi H, Ban Tran H, Tru Huy V, Hong Thi Minh P et al (2022) Development and Validation of Clinical Diagnostic Model for Girls with Central Precocious Puberty: Machine-learning Approaches. PLoS ONE. ;17(1)
22. Pan L, Liu G, Mao X, Li H, Zhang J, Liang H et al (2019) Development of Prediction Models Using Machine Learning Algorithms for Girls with Suspected Central Precocious Puberty: Retrospective Study. JMIR Med Inf 7(1):e11728

Figures

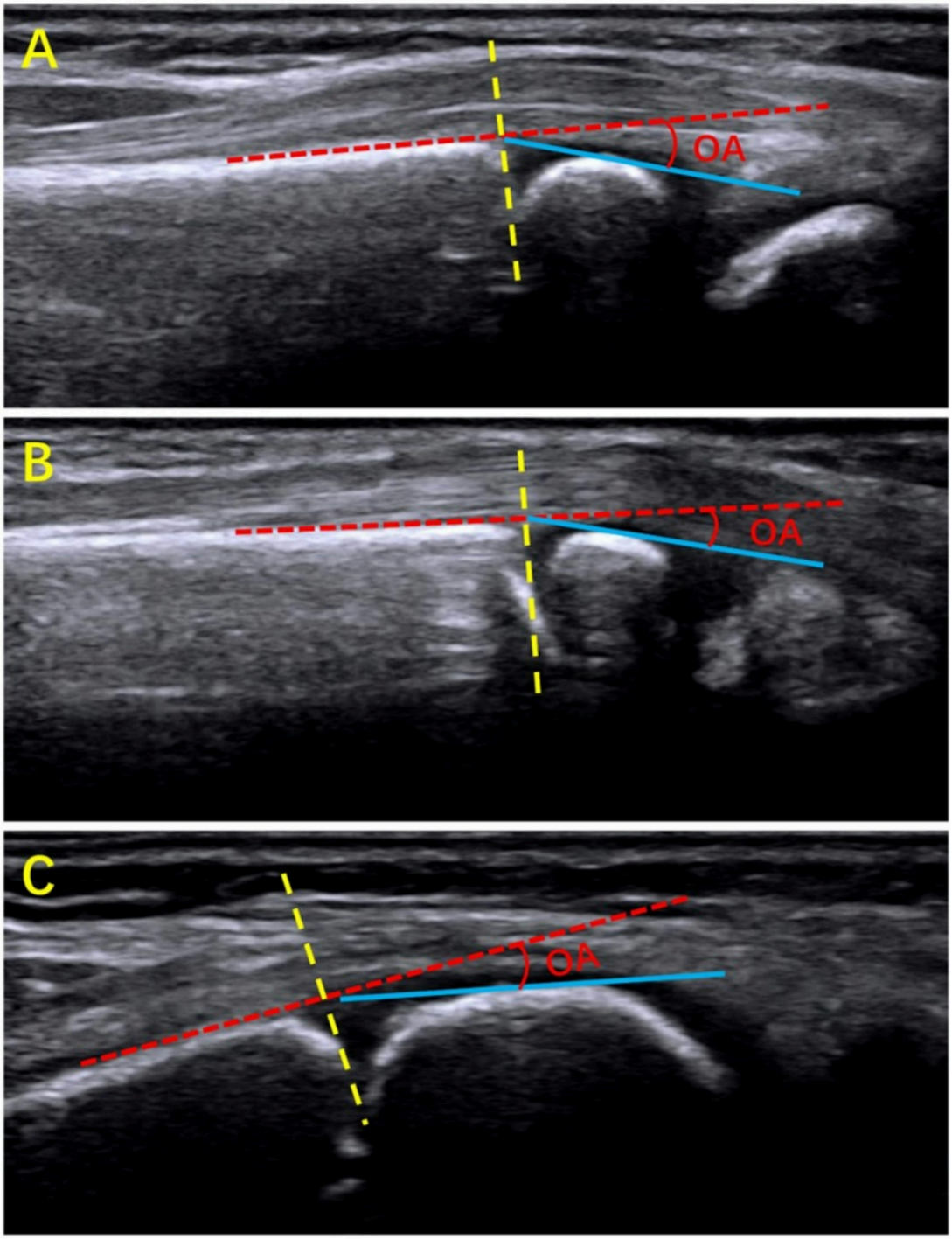


Figure 1

Schematic representation of ossification angle (OA) measurement.

A: Distal radius. B: Distal ulna. C: Distal femur.

The baseline (red line) is drawn along the diaphyseal margin. From the furthest point of the diaphysis, a perpendicular line (yellow line) is dropped to intersect the baseline at the intersection point. A tangent line (blue line) is drawn from the intersection point to the hyperechoic band of the secondary ossification center. The ossification angle (OA) is defined as the angle between this tangent line and the baseline.

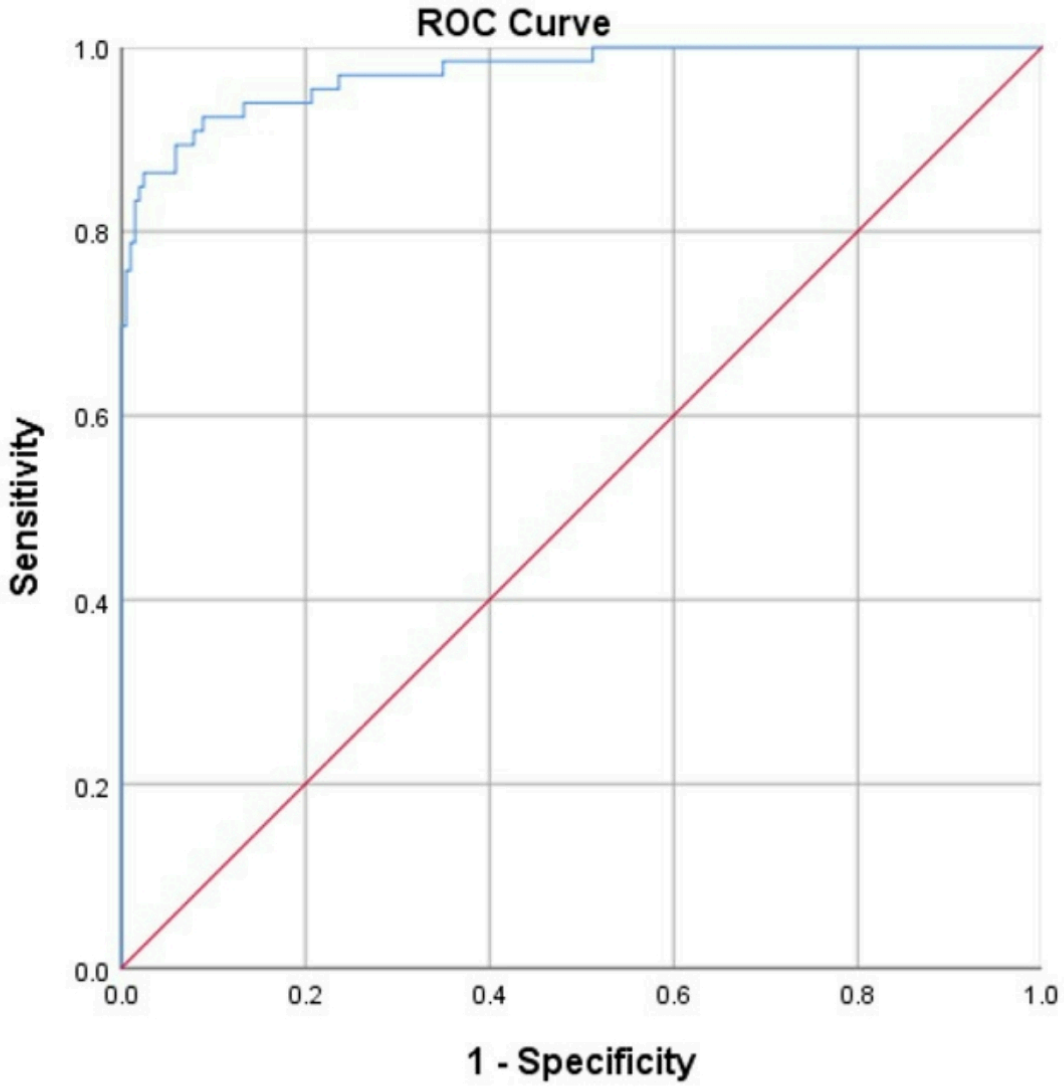


Figure 2

Receiver operating characteristic (ROC) curve of the diagnostic model.

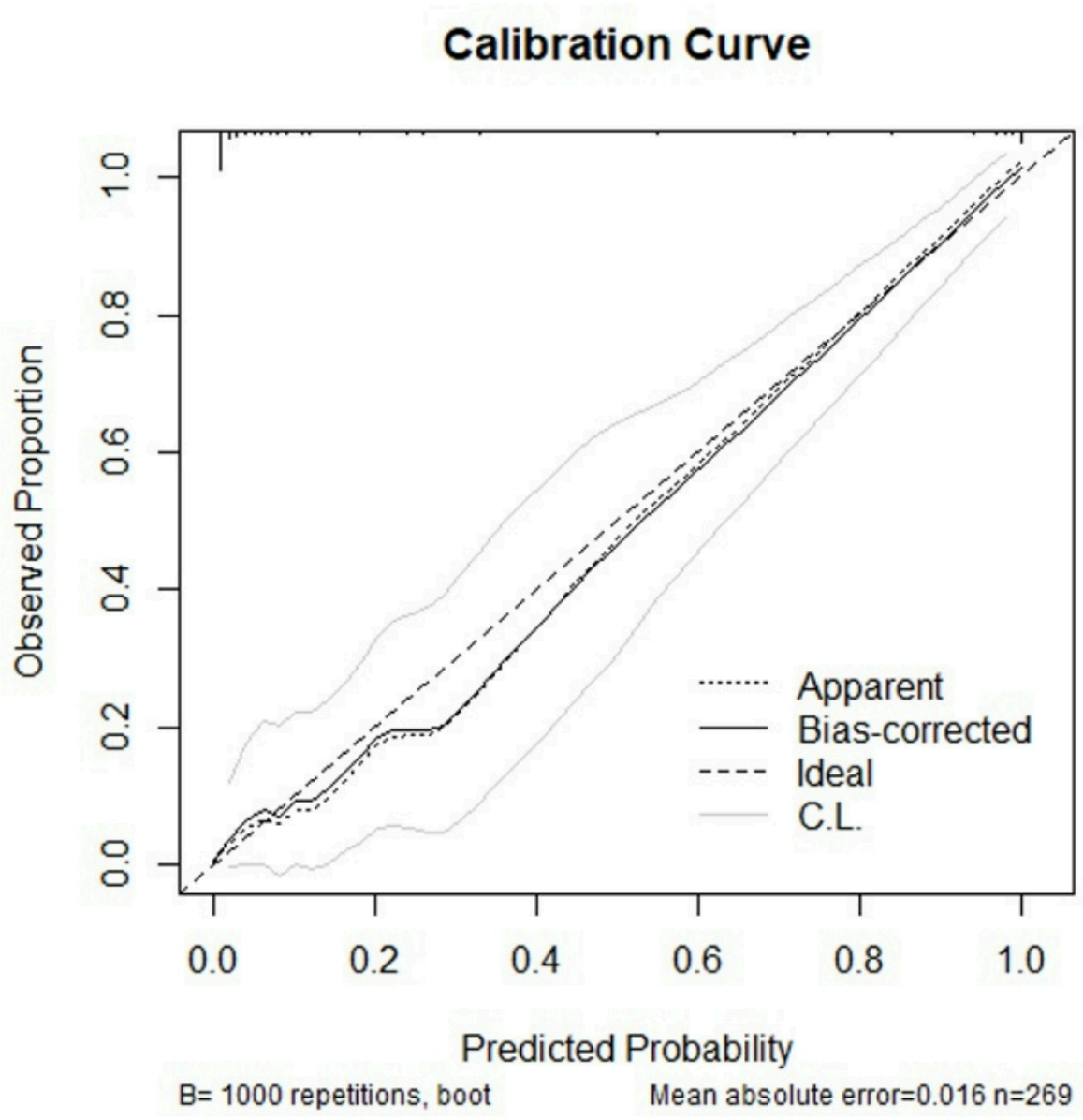


Figure 3

Calibration curve of the diagnostic model.

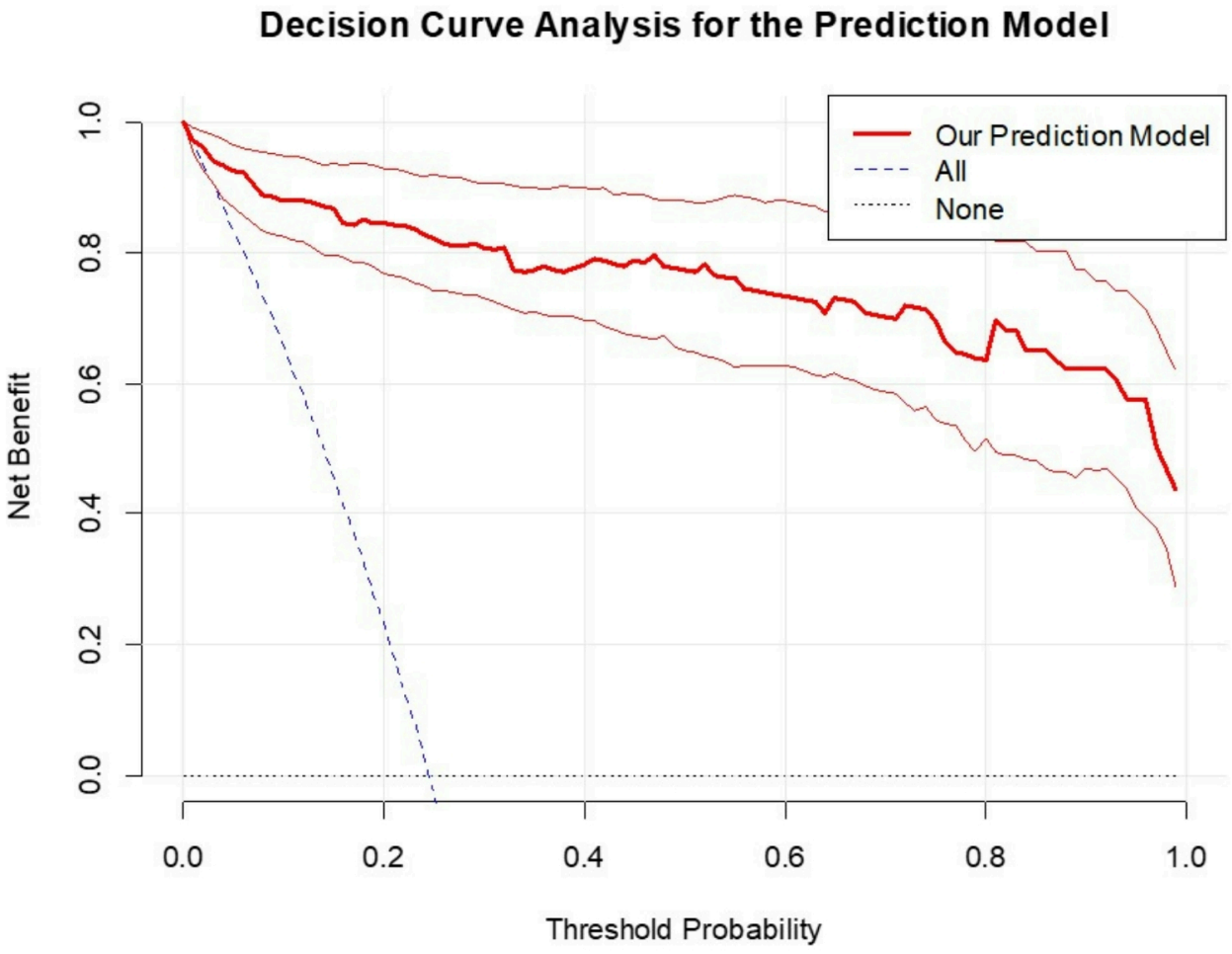


Figure 4

Decision curve analysis (DCA) of the diagnostic model.

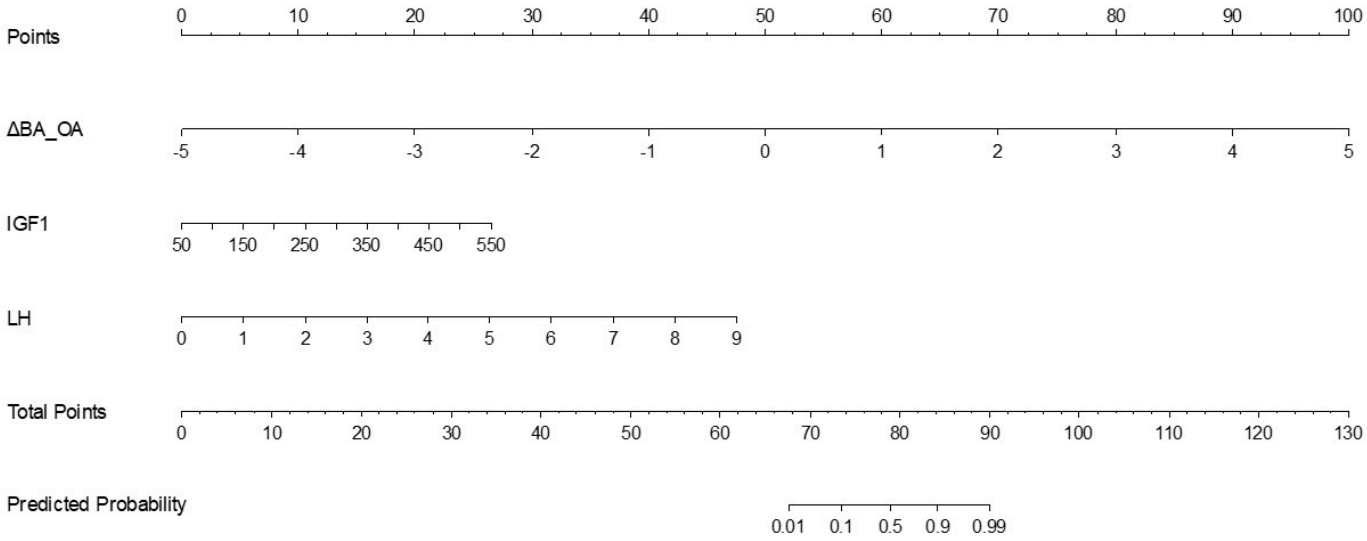


Figure 5

Nomogram for individualized prediction of CPP risk.